Template Growth of Photoconductive Metal−CdSe−Metal Nanowires

David J. Peña,[†] Jeremiah K. N. Mbindyo,[†] Anthony J. Carado,[†] Thomas E. Mallouk,*[,†] Christine D. Keating,*[,†] Baharak Razavi,[‡] and Theresa S. Mayer[‡]

Departments of Chemistry and Electrical Engineering, The Pennsylvania State University, University Park, Pennsylvania 16802

Received: February 18, 2002; In Final Form: May 24, 2002

Metal−CdSe−metal (metal = Au, Ni) nanowires were grown by electrochemical replication of porous aluminum oxide and polycarbonate track etch membranes with pore diameters of 350 and 70 nm, respectively. The lengths of the individual segments of the nanowires were controlled by varying the amount of charge that was passed. The composition of the CdSe segments was characterized by energy-dispersive X-ray spectroscopy. A 1:1 ratio could be obtained, and Cd- and Se-rich stoichiometries were also made by adjusting the concentrations of Cd^{2+} and SeO_2 in the aqueous plating solutions. X-ray powder diffraction showed the presence of both zinc blende and wurzite phases, and grain sizes on the order of 10 nm were observed by TEM. The nanowires were resistive in the dark but showed pronounced visible light photoconductivity.

Introduction

There is growing interest in 1D nanostructures with functional electronic characteristics. The motivations for these studies are the changes in properties that arise from quantum confinement and the potential applications of nanowires in very high density logic, memory, optoelectronic, and sensing devices.[1−4] Most of these applications involve the use of heterostructures in which materials of different compositions meet at interfaces. For example, by crossing n- and p-type semiconductor nanowires, Lieber et al. have made nanoscale rectifiers, field-effect transistors, and light-emitting diodes.[5] Nanowires that are compositionally modulated along their lengths have also been fabricated recently and some show similar electronic and photonic effects.[6−9]

Apart from their potential electronic applications, compositionally modulated semiconductor nanowires are interesting for possible uses in energy conversion (e.g., in p−n junction thermoelectric devices and nanowire array solar cells). Both experimental and theoretical studies indicate that the thermoelectric figure of merit should increase for high aspect ratio nanocrystals of narrow gap semiconductors.[10−12] The availability of both high- and low-temperature routes to nanowires of a growing number of semiconductors suggests that it may be possible to avoid the deleterious effects of grain boundary recombination in photovoltaic and photoelectrochemical devices. Until now, there have been relatively few studies that bear on this question. Photoconductivity has recently been observed in homogeneous InP and ZnO nanowires,[13,14] but to our knowledge, photoeffects in metal−semiconductor nanowire heterostructures have not been studied.

Nanowires of many compositions have been prepared using porous templates as "molds".[15−21] Anodic alumina oxide (AAO) and nuclear track etch polymer membranes are two commonly used templates.[22−25] They have been used to make nanowires composed of metals,[17,20,26,27] semiconductors,[18,28] and polymers.[29,30] This method has recently been used to make CdS, CdSe, CdTe, and AgI nanowires.[16,18,31] The electrical properties of bundles of some of these nanowires were measured and were shown to have some rectification behavior. However, these were single-component wires, and so far their photoconductivity and other photochemical properties have not been explored.

We report here the synthesis of metal−CdSe−metal nanowires by electrochemical replication of AAO and polycarbonate track etch membranes. The semiconductor is sandwiched between Au or Ni segments. Dissolving the template yields a colloidal suspension of free-standing nanowires. The end-on junction between the semiconductor and the metal makes it possible to align these nanowires between metal contact pads and to make contact exclusively to the metal segments. We find that the electronic conductivity of individual CdSe nanowires increases by a factor of 15 when they are illuminated by visible light. The photoconductivity can be switched on and off reversibly by modulating the light.

Experimental Section

Anodisc 25 alumina filtration membranes with a rated pore diameter of 200 nm were purchased from Whatman. Scanning electron microscope (SEM, JEOL 5400) images showed the diameters of replica wires to be 350 nm, indicating that the pores were larger than the rated diameter. Polycarbonate track etch membranes with a rated pore diameter of 30 nm and a measured replica diameter of 70 nm were obtained from Osmonics.

Synthesis of Nanowires in Alumina Membranes. M−CdSe−M nanowires were made by a modification of a method previously described for metal nanowires, as illustrated in Scheme 1.[16,32] Briefly, one side of the AAO membrane was coated with a 5000-Å thick layer of Ag. More Ag was then deposited galvanostatically at 2 mA/cm^2 for 20 min to cover any pores not blocked by the evaporated Ag. The membrane was then assembled in an electrochemical cell with the open pores facing a plating bath, and Ag was deposited into the pores at 0.5 mA/cm^2 for 20 min. Au or Ni was then electrodeposited at the same current density to make 2−3-μm long nanowires (1 h for Au, 2 h for Ni). Plating solutions for Au (Orotemp 24

* Corresponding authors. E-mail: Tom@chem.psu.edu.
[†] Department of Chemistry.
[‡] Department of Electrical Engineering.

10.1021/jp0256591 CCC: $22.00
Published on Web 07/09/2002

SCHEME 1: Template Growth and Release of Au−CdSe−Au Nanowires

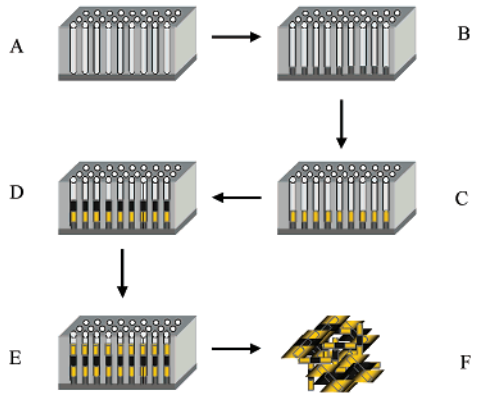

An AAO or polycarbonate template is coated on one side with Ag (A). The template is then filled with approximately 1 μm of Ag (B). An Au segment is then deposited (C), followed by the CdSe layer (D) and another Au layer (E). Finally, the Ag backing and the membrane are dissolved, leaving free-standing nanowires (F).

rack), Ag (1025 Ag bath), and Ni (Ni(S) sulfamate) were from Technic, Inc., Cranston, RI. CdSe plating solutions were made in-house from 0.3 M $CdSO_4$, 0.25 M H_2SO_4, and 0.7 mM SeO_2 as described by Klein et al.[16]

When a metal segment was grown, the electrolyte solution was removed, and the new solution was introduced while holding the current at 0.03 mA/cm^2. This allowed the plating of noble metals onto the silver backing or the CdSe segments without etching of the previously grown layer. CdSe was deposited at ambient temperature using a cyclic voltammetric technique[16]—sweeping the potential from −350 or −400 mV to −800 mV at 750 mV/sec. A saturated calomel electrode (SCE) or a Ag/AgCl electrode was used as a reference. Once the desired length of semiconductor was plated, the electrolyte was changed, and a second metal segment (Au or Ni) was plated on top. Using this method, Au−CdSe−Ni−Au, Au−Ni−CdSe−Ni−Au, and Au−CdSe−Au sequences were made.

The Ag backing was dissolved in 4 M HNO_3, and the nanowires were released by dissolving the alumina membrane in 3 M NaOH. The suspension was centrifuged at ∼2400*g*, and the wires were washed three times with water and twice with ethanol and then suspended in 1 mL of CH_3CH_2OH.

Synthesis of Nanowires in Polycarbonate Membranes. Electrodeposition into the polycarbonate membranes followed a similar procedure using a BAS 100 potentiostat. The reference electrode was SCE, and the counter electrode, a Pt wire. CdSe was electrodeposited from a solution that was 0.6 M $CdSO_4$ and 0.6 mM SeO_2 in 0.5 M H_2SO_4.

Segmented nanowires were made by electrodepositing Au or Ni at −0.90 V versus SCE, followed by CdSe using a CV sweep of 500 mV/s between −350 and −500 mV versus SCE and then finally Au or Ni on top. Electroplating was stopped when the nanopores were filled and metal began to appear on top of the membrane. Any metal that was deposited on top of the membrane was removed with a Kimwipe. The nanowires were released when needed by dissolving the membrane in methylene chloride.

Electrofluidic Alignment of the Nanowires. The ethanolic suspension of 350-nm diameter nanowires was diluted 10:1 with 2-propanol, and individual wires were aligned in an AC electric field as previously described.[33] The 70-nm nanowires were aligned from a suspension in dichloromethane. Electrical measurements were obtained via an HP 4145B semiconductor parameter analyzer by contacting lithographically patterned Au contact pads with W microprobes (Micromanipulator Company, Inc.) on a vibration isolation table.

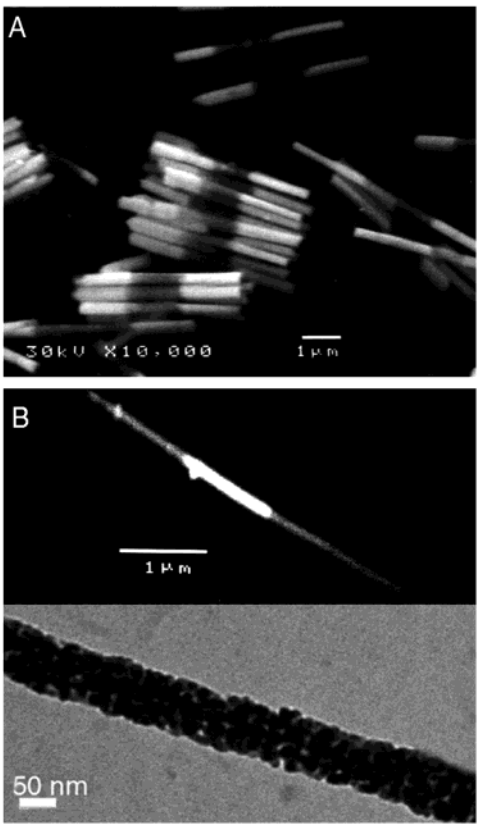

Figure 1. SEM images of 350-nm diameter Au−CdSe−Au nanowires (A) and a 70-nm diameter Ni−CdSe−Ni nanowire (B). The lower panel in (B) shows a higher magnification TEM image of a 70-nm diameter CdSe segment.

Results and Discussion

Figure 1 shows electron micrographs of a 350-nm diameter Au−CdSe−Au nanowires and a 70-nm diameter Ni−CdSe−Ni nanowire. These images show that the nanowires can be removed intact from the template. The scanning electron microscope was operated in secondary electron mode for the larger diameter nanowires and in backscattering mode for the smaller nanowires. CdSe appears darker than Au in the upper image because of the lower energy of the scattered electrons and brighter than Ni in the lower image for the same reason. A transmission electron micrograph (TEM) of a 70-nm diameter CdSe wire shows that it is composed of grains approximately 10-nm in size.

Using the difference in contrast between the metals and CdSe, we found that it was possible to calibrate the growth of the semiconductor segments. Figure 2 shows a plot of CdSe segment length versus the number of cyclic voltammetric scan cycles. Each point in the plot was obtained by averaging the lengths of approximately 50 nanowires in SEM images. From the slope of the line, the average length of CdSe is 2 Å/cycle up to about 10 000 cycles. The length polydispersity increases with the number of scans up to about 25% of the total length at 10 000 scans. In these experiments, the growth reached a plateau after 10 000 scans because of depletion of Se in the solution. By changing the plating solution, it was possible to grow longer segments. However, CdSe segments longer than about 3 μm were easily broken upon release from the membrane, probably

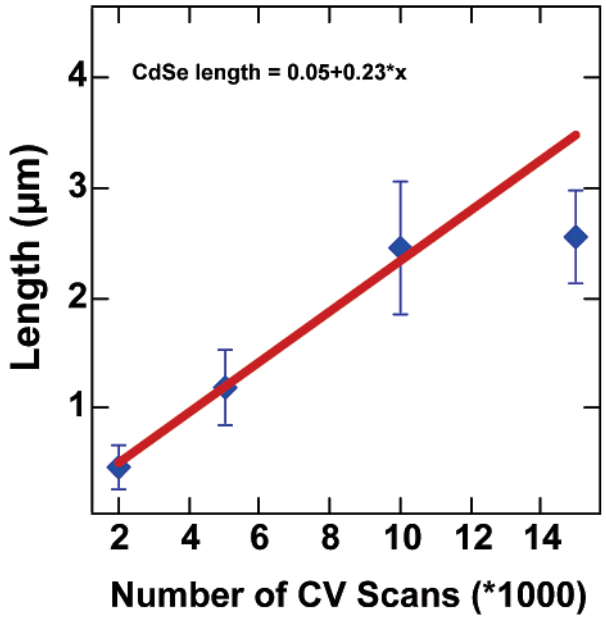

Figure 2. Graph of CdSe segment length vs the number of cyclic voltammetric scans for 350-nm diameter nanowires. Error bars show the standard deviation in length.

TABLE 1: Ratio of Cd to Se as Determined by EDS in a Semiconductor Thin Film as a Function of the Concentration of SeO_2 in the Plating Solution

concentration of SeO_2 (mM)	Cd/Se
0.35	1.0:0.47
0.70	1.0:0.91
1.4	1.0:1.0
2.8	1.0:1.5

because of the brittle nature of the polycrystalline semiconductor.[34]

The electronic properties of compound semiconductors are very sensitive to nonstoichiometry and extrinsic doping.[35] Energy-dispersive X-ray spectroscopy (EDS) was used to determine the effect of changing the concentration of the plating solution on the stoichiometry of electrodeposited CdSe. A 1-μm thick CdSe film was grown on an Au film that had been thermally evaporated on a glass microscope slide. The concentration of the SeO_2 was varied from 0.40−1.4 mM while keeping the $CdSO_4$ concentration constant at 0.30 M. A typical scan of a CdSe sample that was prepared with 0.70 mM SeO_2 solution shows four prominent peaks: Se L at 1.38 keV, Si K at 1.74 keV, Au L at 2.12 keV, and Cd L at 3.14 keV. Because of the high energy of the incident electrons (30 keV), penetration through the CdSe and Au layers occurs, giving rise to a Si peak. The approximate Cd/Se ratio was determined from the relative peak heights in the EDS spectra. As seen in Table 1, the Cd/Se ratio varied from 1.0:0.47 for the 0.35 mM CdSe sample to 1.0:1.5 for the 2.8 mM CdSe sample. An approximately 1.0:1.0 stoichiometry could be obtained with 1.4 mM $CdSO_4$. These experiments show that the stoichiometry of electrodeposited CdSe is quite sensitive to the composition of the plating solution.

An X-ray powder diffraction (XRD) pattern of CdSe nanowires grown in an AAO membrane is shown in Figure 3. A 250-nm Au plug was first plated inside the membrane, and CdSe was then grown from a 0.7 mM SeO_2 solution. The membrane was dissolved with 3 M NaOH without removing the Ag backing, exposing the CdSe nanowires. The etched membrane was fixed to the sample stage so that the long axis of the wires was oriented perpendicularly to the focusing plane of the diffractometer. The peaks in the pattern can be indexed to a mixture of cubic (zinc blende) and hexagonal (wurzite) CdSe phases, along with face-centered cubic Ag. Three minor peaks attributed to AgSCN, which is possibly a byproduct of the silver plating step, are also seen in the pattern. This phase, along with the Ag lines, disappeared when the Ag backing layer was dissolved in nitric acid.

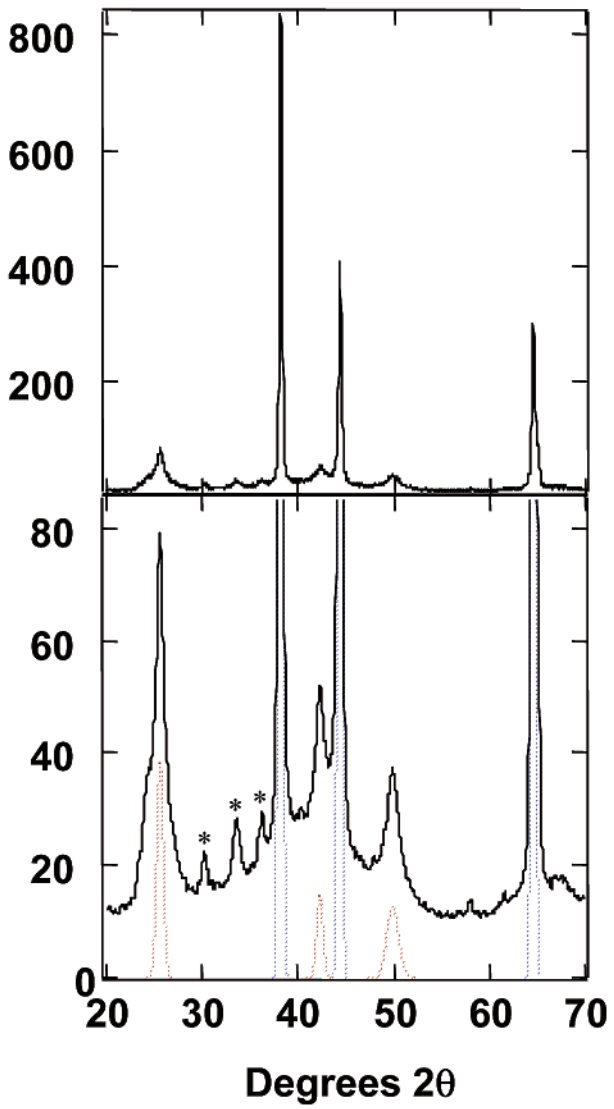

Figure 3. X-ray powder diffraction pattern of a CdSe nanowire array on a silver backing layer after removal of the AAO template. The upper panel shows the pattern at full scale. The lower panel shows a blow up of the pattern, with simulated diffraction lines for Ag (blue) and cubic CdSe (red). Asterisks denote AgSCN peaks.

TABLE 2: XRD Peak Assignments for a CdSe Nanowire Array

angle (2θ) (deg)	d value (Å)	relative intensity	assignment	Miller indices
24.098	3.69	3.3	CdSe	100 hex
25.285	3.48	11.2	CdSe	002 hex
				111 cubic
30.265	2.95	1.1	AgSCN	−202
33.550	2.67	1.5	AgSCN	221
36.225	2.48	1.1	AgSCN	222
38.120	2.36	100.0	Ag	111
42.275	2.14	2.9	CdSe	110 hex
				220 cubic
44.300	2.04	41.8	Ag	200
49.770	1.83	1.8	CdSe	112 hex
				311 cubic
64.430	1.44	21.9	Ag	220

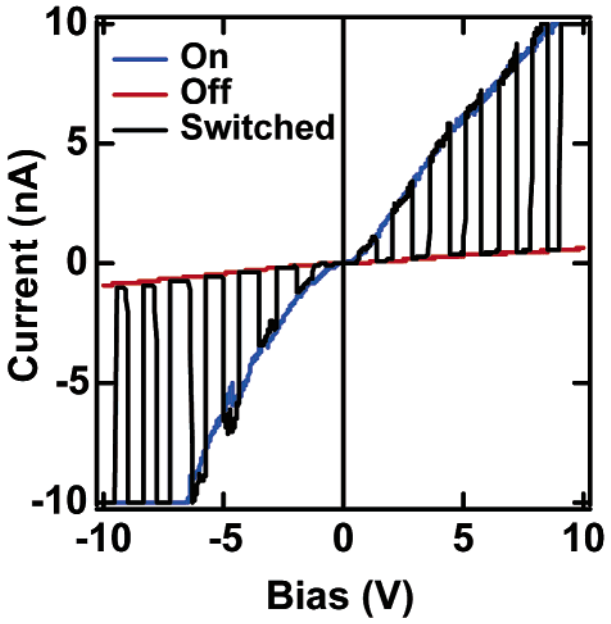

Figure 4. I−V curves of an Au−CdSe−Au nanowire taken in the light and the dark and with the light switched on and off at 5-s intervals during the voltage sweep.

The lower panel in Figure 3 shows a simulated XRD pattern for cubic CdSe mixed with face-centered cubic Ag. Although the CdSe lines are broader than the narrow lines attributed to Ag, the presence of the hexagonal CdSe phase contributes to the peak widths. This makes it difficult to estimate the size of the crystalline CdSe domains from the XRD pattern.[36] Judging from the TEM micrograph in Figure 2, the CdSe particles are significantly smaller than the 300-nm crystallites observed by Klein[16] et al. for CdSe deposited on planar substrates.

Figure 4 shows the I−V characteristics of a single 350-nm diameter Au−CdSe−Au nanowire in the light and dark. Both the light and dark curves are nonlinear with a conductance gap near the origin, as expected for a symmetric device with rectifying contacts between a high work-function metal (Au) and an n-type semiconductor. From the dark currents at ±10 V, an upper bound of ca. 3×10^4 Ω cm can be calculated for the resistivity of the CdSe segment. The curve with higher values of current is a scan from 10 to −10 V under white-light illumination from a microscope objective. A change in conductivity by a factor of about 15 was observed in both the positive and negative branches of the I−V curve when the light was alternately switched on and off. This behavior is consistent with an increase in the number of free carriers in the light, as expected from the optical properties of both bulk and nanoscale CdSe. Similar photoeffects were observed with Ni−CdSe−Ni nanowires and with 70-nm diameter wires of both compositions.

The mechanism of photoconductivity is most likely similar to that observed in polycrystalline and quantum dot CdSe.[37−43] This mechanism consists of direct band-gap excitation, with deep trap states and surface states determining the upper bound of the photoexcitation gain. It is likely that the grain boundaries between nanoparticles in the CdSe segments contribute substantially to this trapping. We are currently investigating the contribution of each of these mechanisms.

Figure 4 shows the effect of switching the light on and off at 5-s intervals while continuously varying the bias between the two contacts. The conductivity rises sharply when the light is switched on and falls when it is switched off. The maximum current under illumination is achieved in about 1 s whereas the decay is more rapid, occurring in ca. 200 μs. This result is consistent with a light-induced increase in the number of free carriers, which are quenched rapidly in the dark through recombination and transport under the applied bias. These transients point to the dominant role of band-gap excitation in the photoconduction mechanism. Similar photoeffects were observed with Ni−CdSe−Ni nanowires and with 70-nm diameter wires of both compositions.

Conclusions

Template electrodeposition provides a route to photoconductive, free-standing metal−semiconductor−metal nanowires. Electrodeposition of CdSe gives polycrystalline nanowire segments, which may be of interest in optical sensing and related applications. The cyclic voltammetric technique gives good control over the length of these segments, and their composition can be controlled by adjusting the composition of the plating bath. In principle, this compositional variation could be used to make ohmic contacts via highly doped semiconductor layers. Because other compound semiconductors can also be grown electrochemically, one can imagine making heterojunction devices by the same technique. One challenge in this work will be to develop techniques (possibly through higher temperature electrodeposition or postsynthesis annealing) for making single-crystal semiconductor segments, which are more likely to have useful electronic and photovoltaic properties.

Acknowledgment. We thank the Division of Chemical Sciences, Office of Basic Energy Sciences, Department of Energy, for support of this work under contract DE-FG02-93-ER14374. C.D.K. and T.S.M. acknowledge support by DARPA and ONR under contract ONR-N00014-98-1-0846.

References and Notes

(1) Xu, D.; Xu, Y.; Chen, D.; Guo, G.; Gui, L.; Tang, Y. *Adv. Mater.* **2000**, *12*, 520−522.
(2) Alivisatos, A. P. *Science (Washington, D.C.)* **1996**, *271*, 933.
(3) Alivisatos, L. *Nature (London)* **2000**, 59.
(4) Lieber, C. M. *Sci. Am.* **2001**, *285*, 58−64.
(5) Huang, Y.; Duan, X.; Wei, Q.; Lieber, C. M. *Science (Washington, D.C.)* **2001**, *291*, 630−633.
(6) Markowitz, P. D.; Zach, M. P.; Gibbons, P. C.; Penner, R. M.; Buhro, W. E. *J. Am. Chem. Soc.* **2001**, *123*, 4502.
(7) Wu, Y.; Fan, R.; Yang, P. *Nano Lett.* **2002**, *2*, 83−86.
(8) Gundiksen, M.; Lauhon, L. J.; Wang, J.; Smith, D. C.; Lieber, C. M. *Nature (London)* **2002**, *415*, 617.
(9) Kovtyukhova, N. I.; Martin, B. R.; Mbindyo, J. K. N.; Smith, P. A.; Razavi, B.; Mayer, T. S.; Mallouk, T. E. *J. Phys. Chem. B* **2001**, *105*, 8762.
(10) Koga, T.; Sun, X.; Cronin, S. B.; Dresselhaus M. S. *Appl. Phys. Lett.* **1999**, *75*, 2438.
(11) Koga, T.; Cronin, S. B.; Dresselhaus, M. S.; Liu, J. L.; Wang, K. L. *Appl. Phys. Lett.* **2000**, *77*, 1490.
(12) Venkatasubramanian, R.; Siivola, E.; Colpitts, T.; O'Quinn, B. *Nature (London)* **2001**, *413*, 597.
(13) Wang, J.; Gudiksen, M. S.; Duan, X.; Cui, Y.; Lieber, C. M. *Science (Washington, D.C.)* **2001**, *293*, 1455−1457.
(14) Kind, H.; Yan, H.; Messer, B.; Law, M.; Yang, P. *Adv. Mater.* **2002**, *14*, 158−160
(15) Kressin, A. M.; Doan, V. V.; Klein, J. D.; Sailor, M. J. *Chem. Mater.* **1991**, *3*, 1015−1020.
(16) Klein, J. D.; Herrick, R. D.; Palmer, D.; Sailor, M. J.; Brumlik, C. J.; Martin, C. R. *Chem. Mater.* **1993**, *5*, 902−904.
(17) Al-Mawlawi, D.; Liu, C. Z.; Moskovits, M. *J. Mater. Res.* **1994**, *9*, 1014−1018.
(18) Routkevitch, D.; Bigioni, T.; Moskovits, M.; Xu, J. M. *J. Phys. Chem.* **1996**, *100*, 14037−14047.
(19) Xu, D.; Shi, X.; Guo, G.; Gui, L.; Tang, Y. *J. Phys. Chem. B* **2000**, *104*, 5061−5063.
(20) Foss, C. A.; Hornyak, G. L.; Stockert, J. A.; Martin, C. R. *J. Phys. Chem.* **1994**, *98*, 2963−2971.
(21) Martin, C. R. *Science (Washington, D.C.)* **1994**, *266*, 1961−1966.
(22) Shingubara, S.; Okino, O.; Sayama, Y.; Sakaue, H.; Takahagi, T. *Jpn. J. Appl. Phys.* **1997**, *36*, 7791−7795.

(23) Brumlik, C. J.; Menon, V. P.; Martin, C. R. *J. Mater. Res.* **1994**, *9*, 1174−1183.
(24) Yi, G.; Schwarzacher, W. *Appl. Phys. Lett.* **2000**, *74*, 1746−1748.
(25) Dubois, S.; Michel, A.; Eymery, J. P.; Duvail, J. L.; Piraux, L. *J. Mater. Res.* **1999**, *14*, 665−671.
(26) Hulteen, J. C.; Martin, C. R. *J. Mater. Chem.* **1997**, *7*, 1075−1087.
(27) Foss, C. A.; Tierney, M. J.; Martin, C. R. *J. Phys. Chem.* **1992**, *96*, 9001−9007.
(28) Xu, D. S.; Xu, Y. J.; Chen, D. P.; Guo, G. L.; Gui, L. L.; Tang, Y. Q. *Chem. Phys. Lett.* **2000**, *325*, 340−344.
(29) Martin, C. R. *Acc. Chem. Res.* **1995**, *28*, 61−68.
(30) Martin, C. R. *Adv. Mater.* **1991**, *3*, 457−459.
(31) Routkevitch, D.; Haslett, T. L.; Ryan, L.; Bigioni, T.; Douketis, C.; Moskovits, M. *Chem. Phys.* **1996**, *210*, 343−352.
(32) Martin, C. R. *Chem. Mater.* **1996**, *8*, 1739−1746.
(33) Smith, P. A.; Nordquist, C. D.; Jackson, T. N.; Mayer, T. S.; Martin, B. R.; Mbindyo, J.; Mallouk, T. E. *Appl. Phys. Lett.* **2000**, *77*, 1399−1401.
(34) *Handbook of Chemistry and Physics*, 1st student ed.; Weast, R. C., Ed.; CRC Press: Boca Raton, FL, 1988.
(35) Pandey, R. K.; Sahu, S. N.; Chandra, S. *Handbook of Semiconductor Electrodeposition*; Marcel Dekker: New York, 1996.
(36) Jenkins, R.; Snyder, R. L. *Introduction to X-ray Powder Diffractometry*; Wiley & Sons: New York, 1996; Vol. 138.
(37) Ginger, D. S.; Greenham, N. C *J. Appl. Phys.* **2001**, *87*, 1361−1368.
(38) Nair, M. T. S.; Nair, P. K. *J. Appl. Phys.* **1993**, *74*, 1879−1884.
(39) Vaitkus, J.; Jasinskaite, R.; Kazlauskiene, V.; Miskinis, J.; Sinius, J.; Zindulis, A. *Thin Solid Films* **2001**, *387*, 212−215.
(40) Leatherdale, C. A.; Kagan, C. R.; Morgan, N. Y.; Empedocles, S. A.; Kastner, M. A.; Bawendi, M. G. *Phys. Rev. B* **2000**, *62*, 2669−2680.
(41) Bakkers, E. P. A.; Roest, A. L.; Marsman, A. W.; Jenneskens, L. W.; Jong-van Steensel, L. I.; Kelly, J. J.; Vanmaekelbergh, D. *J. Phys. Chem. B* **2000**, *104*, 7266−7272.
(42) Wilson, J.; Hawkes, J. F. B. *Optoelectronics*; Prentice Hall: New York, 1989.
(43) Ray, B. *II−VI Compounds*; Pergamon Press: Oxford, U.K., 1969.